Improved endurance behavior of resistive switching in $(Ba, Sr)TiO_3$ thin films with W top electrode

Wan Shen, Regina Dittmann, Uwe Breuer, and Rainer Waser

Citation: Appl. Phys. Lett. **93**, 222102 (2008);
View online: https://doi.org/10.1063/1.3039809
View Table of Contents: http://aip.scitation.org/toc/apl/93/22
Published by the American Institute of Physics

Improved endurance behavior of resistive switching in $(Ba,Sr)TiO_3$ thin films with W top electrode

Wan Shen,[1,2,a] Regina Dittmann,[1,2] Uwe Breuer,[3] and Rainer Waser[1,2]
[1]*Institute of Solid State Research, Research Center Juelich, 52425 Juelich, Germany*
[2]*Juelich-Aachen Research Alliance, Section Future Information Technologies (JARA-FIT), 52425 Juelich, Germany*
[3]*Central Division of Analytical Chemistry, Research Center Juelich, 52425 Juelich, Germany*

(Received 24 September 2008; accepted 6 November 2008; published online 1 December 2008)

We compared the resistive switching performance of barium strontium titanate (BST) thin films with tungsten (W) and platinum (Pt) top electrodes, respectively. The yield, endurance, and reliability were strongly improved for the samples with W top electrode. Whereas the samples with Pt top electrode show a fast drop in the resistance for both high and low resistance states, the devices with W top electrode can be switched for 10^4 times without any obvious degradation. We attribute the improved switching performance to a reversible oxidation and reduction in a WO_x layer at the W-BST interface, which was detected by time-of-flight secondary-ion-mass spectroscopy measurements. © *2008 American Institute of Physics*. [DOI: 10.1063/1.3039809]

Resistive random access memory (RRAM) is one of the most promising candidates for the next generation nonvolatile memory[1,2] and the change in device resistance by applying electric fields has been widely observed from simple binary metal oxide[3–6] to complex perovskite (ABO_3) films.[7–9] Several models have been proposed to explain the mechanism.[10–12] Even though the exact microscopic mechanisms are still under controversial discussion, there exists a general agreement that the migration of oxygen ions under an applied electric field plays a key role.[13] Since oxygen vacancies work as the donors in oxide-based semiconductors, the field driven local accumulation or depletion of oxygen vacancies may be identified with the two resistance states. It has been proposed that the reduction or increase in oxygen vacancies may change the Schottky barrier height at the oxide-electrode interface and will thereby modulate the device resistance.[2,14]

Besides a further elucidation of the switching mechanism, it is of considerable importance for potential RRAM application to improve the yield, stability, and reliability of the resistive switching devices. Bistable switching of up to 10^6 cycles has been reported[15] while most others display fast degradation in hundreds of cycles. In this letter, we compare the resistive switching performance of barium strontium titanate (BST) thin films with platinum (Pt) and tungsten (W) top electrodes, which enables us to draw conclusions to fatigue mechanisms present in resistive switching oxide thin films.

The 80 nm thick $SrRuO_3$ (SRO) bottom electrode and 45 nm 0.2% Mn doped $Ba_{0.7}Sr_{0.3}TiO_3$ were deposited *in situ* at $T=700$ °C and $p=0.25$ mbar on single crystalline (100) oriented $SrTiO_3$ (STO) by pulsed laser deposition. The (00l) oriented epitaxial growth of the bilayers is confirmed by x-ray diffraction measurements. The 100 nm Pt was deposited by magnetron sputtering and 20 nm W was e-beam evaporated and covered by 100 nm Pt in order to avoid the oxidation. The metal films were patterned by lithography and dry etching to areas of 0.04 mm^2 down to 2500 μm^2 to form the top electrodes. The *I-V* characteristics were measured using Agilent semiconductor analyzer B1500A.

All samples reveal low initial resistances, thus no "forming" procedure such as thermal or high voltage treatments, which are prerequisites for the observation of resistive switching in STO single crystals,[12] has to be performed. Figure 1 shows typical examples of *I-V* characteristics of Pt/BST/SRO and W/BST/SRO devices, respectively. The voltage was applied on the top electrode and the SRO bottom electrode was grounded. The *I-V* characteristic of the Pt/BST/SRO sample depicted in Fig. 1(a) shows that the initial state of the sample is low resistance state (LRS), which exhibits linear *I-V* dependence, suggesting a metallic charge carrier transport. The *I-V* branch of the high resistance state (HRS) is strongly nonlinear suggesting a semiconducting, thermally activated charge carrier transport, which was proved by the temperature dependence of the resistance depicted in the inset of Fig. 1(a). After a certain amount of cycles, the *I-V* curve of the Pt/BST/SRO sample [the 100th cycle depicted in Fig. 1(a)] changes its shape and both the LRS and the HRS are semiconducting.

In contrast to Pt/BST/SRO devices, the hysteresis curves of W/BST/SRO devices immediately exhibit a transition between two semiconducting states, as depicted in Fig. 1(b). The inset of Fig. 1(b) shows that both the HRS and LRS are thermally activated. The R_{off}/R_{on} of the metallic to semiconducting transition can reach more than 2×10^3 in some Pt/BST/SRO devices but less than 20 for the W/BST/SRO devices. However, the W/BST/SRO device uniformity is greatly improved and all 40 measured pads show stable resistive switching, which is much higher than the devices with Pt top electrodes, about 58% and 40% as reported previously.[9] The R_{off}/R_{on} of the W/BST/SRO device, readout at 0.5 V, remains about 6 for 1000 cycles, while the R_{off}/R_{on} of the Pt/BST/SRO device already decreases from about 6 to 1.3 after 100 cycles.

Figure 2 displays the pulse measurement of Pt/BST/SRO and W/BST/SRO devices, which were set/read/reset/read for 10^4 times. With further increased number of cycles, the Pt/BST/SRO devices show fast resistance decay in both HRS

[a]Electronic mail: shen@iwe.rwth-aachen.de.

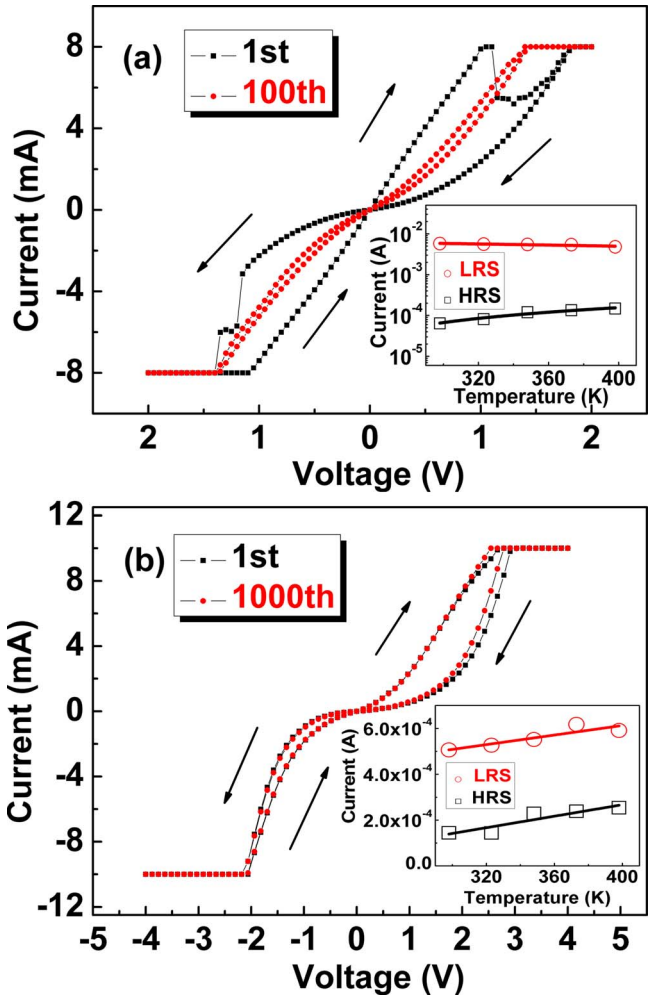

FIG. 1. (Color online) *I-V* curves of (a) Pt/BST/SRO structure and (b) W/BST/SRO structure. The insets show the temperature dependence for both structures.

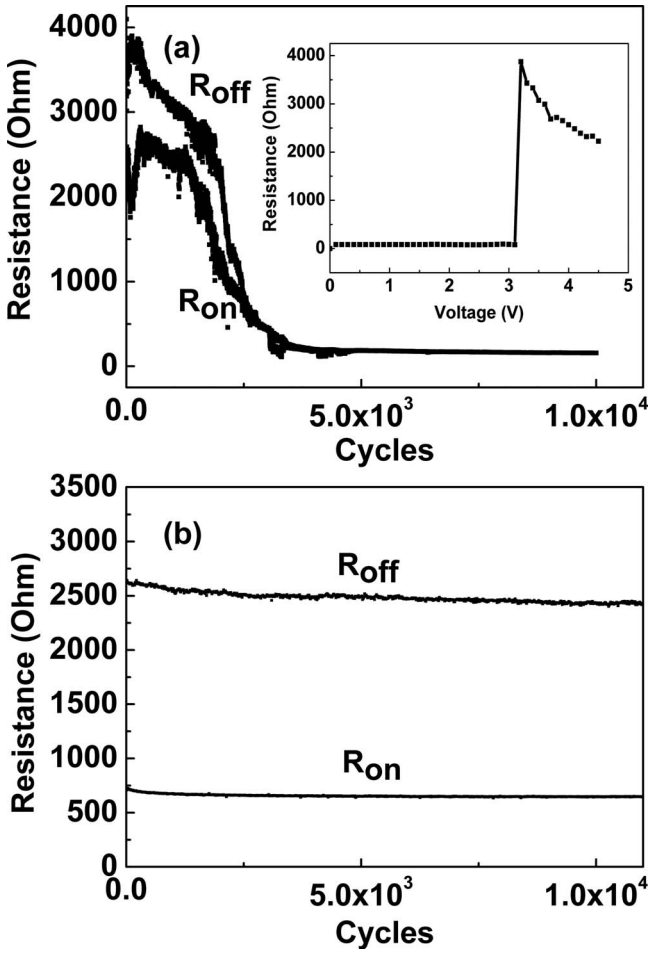

FIG. 2. Pulse measurement of (a) Pt/BST/SRO structure and (b) W/BST/SRO structure. The inset of (a) shows that the fatigued Pt/BST/SRO device can be refreshed to switch back to the HRS. The set and reset voltage is ±4.5 V and the resistances are readout at 0.5 V. The pulse width is 0.1 s.

and LRS and the memory window is closed after 2000 cycles [Fig. 2(a)]. In contrast to this, the reliability of W/BST/SRO device is extraordinarily enhanced and the memory window is well kept after switching for 10^4 times [Fig. 2(b)].

As the work functions of Pt (5.65 eV) and W (4.55 eV) are higher than the electron affinity of BST films (4.1 eV), Schottky barrier is expected for Pt/BST interface, whereas for the W/BST this effect should be less pronounced. Contradictory to the observation, the initial state of the Pt/BST/SRO devices is metallic, which may be attributed to the modification of the interface during sputtering of the Pt film.[16] Furthermore, the observed initial metallic state shows that the as-deposited BST films are oxygen deficient and the BST-SRO interface provides an Ohmic contact. After a few cycles when the oxygen vacancies in the film are redistributed, the Schottky barrier at the Pt-BST interface is recovered and the metallic branch of the *I-V* curve vanishes as depicted in Fig. 1(a).

For W/BST/SRO devices, no initial metallic branch is observed. This may be attributed either to the fact that the e-beam evaporation of the W top electrode preserves the oxygen stoichiometry at the interface or to the formation of an insulating WO_x interface layer at the BST-W interface.

In order to elucidate the interface scenario, we performed time-of-flight secondary-ion-mass spectroscopy (TOF-SIMS) measurements and analyzed the depth profiles of O_2, Ti, and W shown in Fig. 3(a). The most obvious feature in the interface region is the W peak, which has to be attributed to a change in the W sputtering yield in the surface region. Furthermore, it can be clearly seen that the O_2 signal starts to increase simultaneously with the W signal but the rise in Ti signal from the BST layer is delayed for about 6 s. This is a clear hint on the existence of a WO_x layer at the interface because, for an abrupt interface between W and BST, the O_2 signal should rise simultaneously with the Ti signal. By assuming that the WO_x layer has the same etching rate as the W metal, one can estimate the WO_x to be in the order of 1 nm.

To eliminate the possibility that a WO_x layer, which may already be formed during the deposition of the W top electrode, dominates the resistive switching and can exist independent of the BST film, a Pt/W/SRO device was prepared in the same condition as mentioned above. No hysteric *I-V* curve is observed and the device shows Ohmic contact at the interface. It indicates that the interplay between BST and WO_x is responsible for the observed switching phenomena.

The WO_x interface layer may strongly affect the movement of oxygen at the interface, the injection into the top electrode, and finally the exchange of oxygen with the atmosphere. The improved endurance of our samples with W top electrodes is similar to the phenomenon observed in ZrO_2

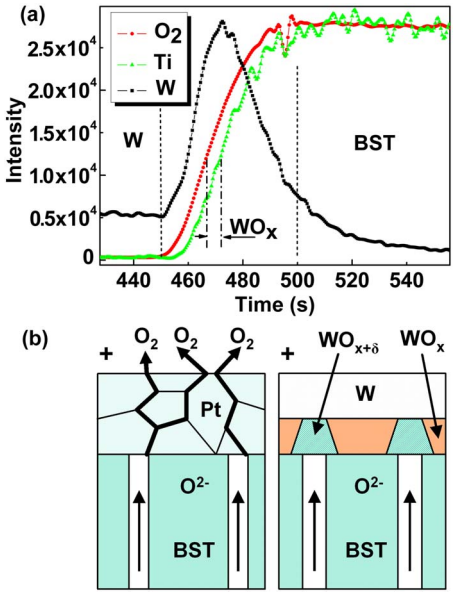

FIG. 3. (Color online) (a) TOF-SIMS of W/BST interface. The W signal is normalized from 1045 and Ti from 240 to the level of the BST bulk regime (O_2 signal). (b) Illustration of switching mechanism when positive bias is applied on the top electrode for Pt/BST/SRO and W/BST/SRO structures.

films with Ti top electrode[5] and $La_{0.7}Ca_{0.3}MnO_3$ films with samarium (Sm) top electrode,[17] which were also attributed to the existence of a metal oxide layer formed at the interface acting as source and sink for oxygen vacancies.

In order to understand the fatigue behavior of samples with Pt top electrode shown in Fig. 2(a), one should regard the movement of oxygen vacancies under an applied electric field. When the positive bias is applied on the Pt top electrode, the oxygen vacancies are repelled from the interface and the device is switched to HRS. When the negative bias is applied, the oxygen vacancies are pushed back to the interface and result in LRS. According to the diffusion of oxygen along the Pt grain boundaries,[18] additional oxygen vacancies could be injected from the anode into the BST film during cycling,[19] as sketched in Fig. 3(b), and may cause the degradation depicted in Fig. 2(a). It is reasonable to deduce for BST films that the endurance should be improved in a highly oxygenating environment or when a diffusion barrier,[20] such as TaSiN used in dynamic random access memory, is introduced in order to block the oxygen infusion to the atmosphere. Moreover, the inset of Fig. 2(a) shows that the fatigued Pt/BST/SRO device can be refreshed to the HRS again, which indicates that the oxygen is supplied from the sample interior most likely from the SRO bottom electrode, and thereby the Schottky barrier is recovered.

In case of W/BST/SRO devices, the resistance of the interface WO_x layer can be increased by reducing the number of oxygen vacancies.[21] When a positive bias is applied on the W top electrode, the positively charged oxygen vacancies are repelled from W/BST interface, the WO_x layer is further oxidized to $WO_{x+\delta}$, and the resistance increases. In reversed electric field, the oxygen can be released from the $WO_{x+\delta}$ layer, the resistance of the $WO_{x+\delta}$ layer decreases, and the oxidation state of the $WO_{x+\delta}$ is reduced. Thus the WO_x interface layer works like an oxygen sink and it stores and releases the oxygen during switching.

Even though the resistive switching in our samples is strongly dominated by the interface, we did not find any pad size dependence in the area range we measured. Therefore, we conclude that in case of our switching samples have filamentary characters. The conductive filaments may be connected and disconnected at the interface through the reduction and oxidation of the WO_x layer, respectively, at the end of the filaments as sketched in Fig. 3(b).

In conclusion, the yield, endurance, and reliability were improved by using W top electrode, which attribute to the reversible oxidation and reduction in a WO_x layer existing at the interface between W top electrode and BST film. The device with W top electrode can switch 10^4 times without obvious degradation and the memory window is well kept. The switching behavior can be explained by the oxygen vacancy migration to connect/disconnect the conductive filaments at the interface.

We thank Tobias Menke for helpful discussions and the critical reading of the manuscript. This work was financially supported by Intel, Inc., Santa Clara.

[1] R. Waser and M. Aono, Nature Mater. **6**, 833 (2007).
[2] A. Sawa, Mater. Today **11**, 28 (2008).
[3] C. B. Lee, B. S. Kang, M. J. Lee, S. E. Ahn, G. Stefanovich, W. X. Xianyu, K. H. Kim, J. H. Hur, H. X. Yin, Y. Park, and I. K. Yoo, Appl. Phys. Lett. **91**, 082104 (2007).
[4] A. Chen, S. Haddad, Y. C. Wu, Z. Lan, T. N. Fang, and S. Kaza, Appl. Phys. Lett. **91**, 123517 (2007).
[5] C. Y. Lin, C. Y. Wu, C. Y. Wu, T. Y. Tseng, and C. Hu, J. Appl. Phys. **102**, 094101 (2007).
[6] B. J. Choi, D. S. Jeong, S. K. Kim, C. Rohde, S. Choi, J. H. Oh, H. J. Kim, C. S. Hwang, K. Szot, R. Waser, B. Reichenberg, and S. Tiedke, J. Appl. Phys. **98**, 033715 (2005).
[7] S. Q. Liu, N. J. Wu, and A. Ignatiev, Appl. Phys. Lett. **76**, 2749 (2000).
[8] A. Beck, J. G. Bednorz, Ch. Gerber, C. Rossel, and D. Widmer, Appl. Phys. Lett. **77**, 139 (2000).
[9] R. Oligschlaeger, R. Waser, R. Meyer, S. Karthäuser, and R. Dittmann, Appl. Phys. Lett. **88**, 042901 (2006).
[10] M. J. Rozenberg, I. H. Inoue, and M. J. Sanchez, Phys. Rev. Lett. **92**, 178302 (2004).
[11] T. Fujii, M. Kawasaki, A. Sawa, H. Akoh, Y. Kawazoe, and Y. Tokura, Appl. Phys. Lett. **86**, 012107 (2005).
[12] K. Szot, W. Speier, G. Bihlmayer, and R. Waser, Nature Mater. **5**, 312 (2006).
[13] Y. B. Nian, J. Strozier, N. J. Wu, X. Chen, and A. Ignatiev, Phys. Rev. Lett. **98**, 146403 (2007).
[14] J. Yang, M. D. Pickett, X. M. Li, D. A. A. Ohlberg, D. R. Stewart, and R. S. Williams, Nat. Nanotechnol. **3**, 429 (2008).
[15] D. J. Seong, M. Jo, D. Lee, and H. Hwang, Electrochem. Solid-State Lett. **10**, H168 (2007).
[16] S. Ezhilvalavan and T. Y. Tseng, Mater. Chem. Phys. **65**, 227 (2000).
[17] M. Hasan, R. Dong, H. J. Choi, D. S. Lee, D. J. Seong, M. B. Pyun, and H. Hwang, Appl. Phys. Lett. **92**, 202102 (2008).
[18] R. Schmiedl, V. Demuth, P. Lahnor, H. Godehardt, Y. Bodschwinna, C. Harder, L. Hammer, H.-P. Strunk, M. Schulz, and K. Heinz, Appl. Phys. A: Mater. Sci. Process. **62**, 223 (1996).
[19] R. Waser, T. Baiatu, and K. H. Haerdtl, J. Am. Ceram. Soc. **73**, 1645 (1990).
[20] T. Hara, T. Kitamura, M. Tanaka, T. Kobayashi, K. Sakiyama, S. Onishi, K. Ishihara, J. Kudo, Y. Kino, and N. Yamashita, J. Electrochem. Soc. **143**, L264 (1996).
[21] M. Gillet, C. Lemire, E. Gillet, and K. Aguir, Surf. Sci. **532**, 519 (2003).